Appl Microbiol Biotechnol (2008) 79:605–616
DOI 10.1007/s00253-008-1457-7

A conserved Hpa2 protein has lytic activity against the bacterial cell wall in phytopathogenic *Xanthomonas oryzae*

Jiahuan Zhang · Xiaoyu Wang · Yan Zhang · Guiying Zhang · Jinsheng Wang

Received: 1 February 2008 / Revised: 10 March 2008 / Accepted: 11 March 2008 / Published online: 23 April 2008

Abstract The type III secretion system (TTSS) proteins form a needle-like structure injecting effector proteins into eukaryotic target cells. Although the TTSS forms an important pathway for bacterium–host interaction, its assembly process in vivo is poorly understood. The process is thought to include the opening of a pore before TTSS proteins are inserted into the bacterial cell wall. The proteins that break the bacterial cell wall have not yet been identified. We hypothesize that a hypersensitive response and pathogenicity (*hrp*) gene functions to digest the bacterial cell wall because it contains a conserved protein sequence similar to lytic transglycosylase. In this study, we cloned *hrp*-associated 2 (*hpa2*) genes from the bacteria *Xanthomonas oryzae* pathovars. We show in vitro that expressed Hpa2 protein has a lytic activity against bacterial cell walls. The analysis of a loss-of-function mutant of the *hpa2* gene suggests that the *hpa2* affects bacterial proliferation in host plants and a hypersensitive response in nonhost plants. As this is the first of such enzyme activity identified in the Hrp protein family, we speculate that the Hpa2 contributes to the assembly of the TTSS by enlarging gaps in the peptidoglycan meshwork of bacterial cell walls.

Keywords *Xanthomonas oryzae* · *hrp*-conserved · Type III secretion system · Soluble lytic transglycosylase · *hrp*-associated · Plant-inducible promoter

J. Zhang · X. Wang · Y. Zhang · G. Zhang · J. Wang (✉)
Department of Plant Pathology, Nanjing Agricultural University, Weigang 1,
Nanjing 210095, China
e-mail: wangjsh@njau.edu.cn

Introduction

The phytopathogenic bacterium *Xanthomonas oryzae*, including *X. oryzae* pv. *oryzae* (*Xoo*) and *X. oryzae* pv. *oryzicola* (*Xooc*), causes bacterial leaf blight and streak in rice (Kumar and Sakthivel 2001; Horino 2002; Niño-Liu et al. 2006; Zhao et al. 2004). These bacterial strains possess a type III secretion system (TTSS) to transport effector proteins directly from the bacterial cytoplasm into eukaryotic target cells (Hueck 1998). The TTSS is a pivotal system involved in the secretion of hypersensitive response (HR) and pathogenicity (Hrp) proteins in many species of phytopathogenic bacteria (Galán and Collmer 1999).

The Hrp protein family includes approximately 26 proteins, and its genes are located in stereotypic clusters in several bacterial genomes. In the genomes of *Xoo* strain KACC10331 (Lee et al. 2005) and MAFF 311018 (Ochiai et al. 2005), the *hrp* cluster involves multiple transcripts, including *hrp*-associated (*hpa*) and *hrp*-conserved (*hrc*) genes (Lee et al. 2005; Ochiai et al. 2005; Kim et al. 2003; Sugio et al. 2005). It is interesting to note that plant-inducible promoters (PIPs, containing TTCGC-N_{15}-TTCGC) are identical in four *hrp* operons and similar in three others (last base C substitution in the TTCGC region or changes in the N_{15} region; Oku et al. 2004). This promoter similarity may indicate cooperatively regulated gene expression or function among these genes. Similar to *Xoo* strains, the *Xooc* RS105 genome also contains a cluster of ten *hrp*, nine *hrc*, and eight *hpa* genes and seven regulatory PIP boxes (Zou et al. 2006).

Some Hpa proteins are required for the interaction between the TTSS and the host. HpaB protein from *Xanthomonas campestris* pv. *vesicatoria* (*Xcv*) acts as an exit control protein in type III-dependent protein secretion, which promotes the secretion of a large set of effector

proteins and prevents the delivery of noneffectors into plant cells (Büttner et al. 2004). The HpaA protein from *Xcv* acts as an effector, which may be translocated into the host cell via the TTSS (Huguet et al. 1998) and is required for the HR and full pathogenicity (Gürlebeck et al. 2006). Thus, the Hpa protein is an important factor during bacterium and plant interactions and may play a significant role with regard to pathogenicity.

A *hpa2* deletion mutant with a truncated *hpa1* reduces disease symptoms in *Xoo*, accompanied by a reduced bacteria population in rice leaves (Zhu et al. 2000). The *hpaH* (*hpa2* homologue) mutant in *Xanthomonas axonopodis* pv. *glycines* loses the ability to elicit HR in some nonhosts but had no effect in the others (Kim et al. 2003). It is interesting to note that Hpa2 has a similar sequence to lytic transglycosylase (LT), which may function in opening the bacterial cell wall for the assembly of the TTSS (Koraimann 2003). To test this hypothesis, we cloned *hpa2* genes from five *X. oryzae* pathovars, expressed one Hpa2 protein, and then observed its lytic effect against the cell walls of several stains of bacteria. We reasoned that the phenotype of the *hpa2* mutant may be related to the malfunction in the TTSS. To our knowledge, this is the first report of a Hpa protein in a phytopathogenic bacterium that possesses lytic activity against the bacterial cell walls.

Materials and methods

Bacterial strains, plasmids, and growth conditions

Bacterial strains and plasmids used in this study are described in Table 1. *Bacillus subtilis* and *Escherichia coli* DH5α or BL21 (DE3) strains were grown in Luria–Bertani broth liquid (LB) or Luria-Bertani broth agar medium at 37°C. *Xoo* PXO99^{A}, *Xoo* JXOIII, *Xoo* ZHE173, *Xooc* RS105,

Table 1 Bacterial strains and plasmids used in this study

Strains or plasmids	Relevant genotype or characteristics	Sources or reference
Strains		
E. coli		
DH5α	F^{-} *recA lacZ*M15; hosts of pUC18-T, pUC19-T, pRFR034, and their derivatives	Wang et al. 2007
BL21(DE3)	*lacUV5-T7gene1*; hosts of pET-30a(+) and its derivative	Wang et al. 2007
S17-1 λpir	Containing λ*pir* gene encoding the p protein for the R6K origin of replication	NCCB
X. oryzae. pv.		
oryzae PXO99^{A}	5-Azacytidine resistant, Rif^{r}; Gram-negative bacteria	Li et al. 2004
oryzae JXOIII	Wild-type strain, Rif^{r}; Gram-negative bacteria	Li et al. 2004
oryzae ZHE173	Wild-type strain, Rif^{r}; Gram-negative bacteria	This study
oryzicola RS105	Wild-type strain, Rif^{r}; Gram-negative bacteria	Li et al. 2004
oryzicola HAN1	Wild-type strain, Rif^{r}; Gram-negative bacteria	This study
M. luteus	Gram-positive bacteria; norm substrate of lysozyme	BCCM
B. subtilis	Gram-positive bacteria	This study
C. michiganense subsp. *sepedonicum*	Gram-positive bacteria	This study
564-6	Hpa2 expression strain; derivative of strain bearing pET-30a(+), Km^{r}	This study
464–16	*hpa2* mutant; derivative of *Xoo* PXO99^{A}, Rif^{r}, Cm^{r}	This study
712–22	*hpa2* complement; bearing pUFRcom712-22, Rif^{r}, Km^{r}, Cm^{r}	This study
Plasmids		
pMD18-T	Derivative of vector pUC18, Amp^{r}	TaKaRa (Dalian)
pMD19-T	Derivative of vector pUC19, Amp^{r}	TaKaRa (Dalian)
pMhpa2J	Derivative of pMD18-T, containing *hpa2* fragment from *Xoo* JXOIII	This study
pMhpa2P	Derivative of pMD19-T, containing *hpa2* fragment from *Xoo* PXO99^{A}	This study
pMhpa2ZH	Derivative of pMD19-T, containing *hpa2* fragment from *Xoo* ZHE173	This study
pMhpa2R	Derivative of pMD18-T, containing *hpa2* fragment from *Xooc* RS105	This study
pMhpa2HA	Derivative of pMD19-T, containing *hpa2* fragment from *Xoo* HAN1	This study
pMorf564P	Derivative of pMD19-T, containing *hpa2* ORF fragment of 564 bp	This study
pET-30a(+)	Multiple cloning sites; pBR322 origin Kan coding sequence f1 origin	Novagen
pEorf564P	Derivative of vector pET-30a (+), containing *hpa2* ORF fragment of 564 bp	This study
pMD464	Derivative of pMD19-T, containing a 464-bp fragment in *hpa2* gene	This study
pKNOCK-Cm	containing R6K origin of replication; Cm^{r}; the pBluescript II polylinker	NCCB
pKNO464-16	Derivative of pKNOCK-Cm, containing 464-bp fragment in *hpa2* gene	This study
pMD712	Derivative of pMD19-T, containing complete *hpa2* gene of 712 bp	This study
pUFR034	*IncW*, *Mob(p)*, *Mob*$^{+}$, *LacZa*$^{+}$, PK2 replicon, cosmid, Km^{r}	NCCB
pUFRcom712-22	Derivative of pUFR034, containing complete *hpa2* gene of 712 bp, Km^{r}	This study

Xooc HAN1, and *Clavibacter michiganense* subsp. *sepedonicum* (*Cms*) strains were grown in nutrient broth agar (NA) or nutrient broth liquid (NB) medium at 28°C. The *Micrococcus luteus* (synonym, *Micrococcus lysodeikticus*) strain was grown in NA (Oxoid CM3) solid or liquid medium, as recommended by the Belgian Coordinated Collections of Micro-organism (BCCM), at 30°C. Antibiotics were used at the following concentrations: ampicillin (Amp), 100 μg ml^{-1}; rifampin (Rif), 50 μg ml^{-1}; chloramphenicol (Cm), 20 μg ml^{-1}; kanamycin (Km), 50 (pET-30a (+)) or 25 μg ml^{-1} (pUFR034).

DNA manipulations

Genomic deoxyribonucleic acid (DNA) was prepared using the Bacterial Genomic DNA Mini-prep Kit (V-gene Biotechnology Limited). Plasmids and fragment DNAs were extracted and purified with the Plasmid Mini, Gel Extraction, and Cycle-Pure Kits (Omega Bio-tek). Oligonucleotide primers, restriction endonucleases, and T4 DNA ligase were obtained from TaKaRa (Dalian). All methods were performed according to the suppliers' instructions.

Sequence analyses

Sequences were analyzed using the DNASTAR software and the online at the National Center for Biotechnology Information website (http://www.ncbi.nlm.nih.gov/). Sequence alignment and domain searches were performed with the CLUSTAL W software (1.83), a program available online at European Molecular Biology Laboratory—European Bioinformatics Institute (http://www.ebi.ac.uk/clustalw/) or the Sanger Institute Pfam website (http://www.sanger.ac.uk/Software/Pfam/).

Construction of vectors

Five strains of *Xoo* PXO99^{A}, *Xoo* JXOIII, *Xoo* ZHE173, *Xooc* RS105, and *Xooc* HAN1 were grown in NA or NB media containing Rif for 48 h. Genomic DNAs were extracted using the Bacterial Genomic DNA Mini-prep Kit. Five fragments, including the *hpa2* genes, were amplified by polymerase chain reaction (PCR) using primers hpa2F (5′-TGC CGC CAT CTT GCG TGA CCC TAC-3′) and hpa2R (5′-GCT TTT TTC GCT TGC CCG TT-3′) with an initial denaturation at 95°C for 5 min, 30 cycles of denaturation at 95°C for 30 s, annealing at 55°C for 45 s, and extension at 72°C for 45 s, followed by a final extension at 72°C for 7 min. The PCR products were cloned into pMD19-T or pMD18-T, yielding pMhpa2P, pMhpa2J, pMhpa2ZH, pMhpa2R, and pMhpa2HA, respectively. The cloned fragments were verified by enzyme digestion and sequencing.

A 564-bp open reading frame (ORF) from *Xoo* PXO99^{A} *hpa2* was amplified by PCR from the pMhpa2P using primers Hpa2pETF (5′-GGG G*CA TAT* GAT CAA TTC AAC GAT C-3′) and Hpa2pETR (5′-CGC *GGA TCC* CTA TTC ACC AAT CAC A-3′; *Nde*I and *Bam*HI sites in italics), with the PCR conditions listed above, except that annealing at 60°C. The product was cloned into pMD19-T, yielding pMorf564. Then, pMorf564 and pET-30a(+) were digested with *Nde*I and *Bam*HI. Finally, the 564-bp ORF of the *hpa2* gene was ligated into pET-30a(+) at the same enzyme sites, yielding the expression vector pEorf564P. The pEorf564P was transformed into *E. coli* BL21 (DE3), yielding expression strain 564-6. The *hpa2* ORF was verified by enzyme digestion and sequencing.

A 464-bp fragment of the *hpa2* gene was amplified by PCR from the pMhpa2P using primers 464S (5′-ATG *GAA TTC* TCA ACG ATC GCA TGC C-3′) and 464A (5′-GCC *CTC GAG* TTA CCA TAT TTA TTG G-3′; *Eco*RI and *Xho*I sites in italics), with the PCR conditions listed above, except that annealing was performed at 60°C. The PCR product was cloned into pMD19-T, yielding pMD464. Then, the pMD464 and the suicide plasmid pKNOCK-Cm were digested with *Eco*RI and *Xho*I, and the 464-bp fragment was ligated into pKNOCK-Cm at the same enzyme sites, yielding mutation vector pKNO464-16. Finally, pKNO464-16 was transferred into *Xoo* PXO99^{A} by electroporation, yielding mutation strain 464-16. The vector and mutant were confirmed by PCR and sequencing. Primers Cm660F (5′-ATG GAG AAA AAA ATC ACT GGA TAT A-3′) and Cm660R (5′-TTA CGC CCC GCC CTG CCA CTC ATC G-3′) were used with the PCR conditions above for the detection of the Cm acetyltransferase gene, conferring resistance to Cm.

A complete *hpa2* gene of 712 bp, containing the promoter region, was amplified from the pMhpa2P by PCR using primers Com712F (5′-GCA *TCT AGA* TTC GCT TGC CCG TTA A-3′) and Com712R (5′-TTC *AAG CTT* CTA TTC ACC AAT CAC A-3′; *Xba*I and *Hin*dIII sites in italics) with the PCR conditions above. The PCR product was cloned into pMD19-T, yielding pMD712. Then, the pMD712 and pUFR034 were digested with *Xba*I and *Hin*dIII. Finally, the 712-bp fragment was cloned into pUFR034 at the same enzyme sites, yielding complement vector pUFR712-22. Finally, pUFR712-22 was transferred into the mutation strain 464-16 by electroporation, yielding transformant 712-22, resistant to Cm and Km. The constructed vector was verified by enzyme digestion and sequencing.

Hpa2 protein expression and SDS-PAGE

The expression strain 564-6 was grown overnight in optimal media. The cultures were transferred to LB medium

for 3 h and then induced by the addition of 5.0 mM isopropyl-β-D-thiogalactopyranoside (IPTG; final concentration). Aliquots of culture (100 ml) were harvested (5,000 rpm, 5 min). Pellets were resuspended in 4 ml Tris–ethylenediamine tetraacetic acid (TE) buffer (pH 10.1; 20% [*w*/*v*]), and phenylmethanesulfonyl fluoride was added (final concentration 0.1 mM). The aliquots were sonicated five times with 15-s pulses each time and 20 s between pulses on ice. The sonicates were centrifuged (12,000 rpm, 15 min, 4°C). *E. coli* BL21 (DE3) cells harboring the vector pET-30a(+) were subjected to the same protocol, and the sample was named pET-30a(+) supernatant. All sample supernatants were stored at −20°C or 4°C.

The supernatant samples were analyzed by sodium dodecyl sulfate (SDS) polyacrylamide gel electrophoresis (PAGE; 15% separating and 5% stacking gels; Sambrook and Russell 2001). Aliquots (20 μl) of the supernatant samples were mixed with 20 μl of twofold loading buffer (20 μl; 100 mM Tris–HCl, pH 6.8, 200 mM β-mercaptoethanol, 4% [*w*/*v*] SDS, 0.2% [*w*/*v*] bromophenol blue, 20% [*v*/*v*] glycerol). The gel was then stained with Coomasie brilliant blue R250.

The expressed protein concentration in the supernatant, measured with the BCA-100 protein quantitative analysis kit (Shenergy Biocolor BioScience & Technology), was initially 50.0 mg ml^{-1}. The concentration of the protein (named as Hpa2) in the supernatant, encoded by the *hpa2* gene ORF from the *Xoo* $PXO99^A$ strain, was determined at 19.6 mg ml^{-1} according to band analysis and the measured values. SDS-PAGE bands were analyzed using the SCAN BAND software.

Secretion analysis

Strains *M. luteus* and 564-6 were cultured to an optical density (OD_{600}) of 7.0 in LB medium. Aliquots (500 μl) of the two cell suspensions were added to 1.5-ml microcentrifuge tubes, and then, as controls, 1-ml aliquots of each strain were added to the tubes. Total protein including Hpa2 was 5.0 mg ml^{-1} and for IPTG, 5.0 mM (final concentrations). All solutions were adjusted to an OD_{600} of 7.0 and kept at 28°C for 12 h. OD_{600} values were then measured.

Investigation of the lysis phenotype

Six strains, *M. luteus*, *B. subtilis*, *Cms*, *E. coli*, *Xoo* $PXO99^A$, and *Xooc* RS105, were grown in optimal media and at appropriate temperatures. After they were harvested, the cells were resuspended in TE buffer (pH 6.8). Aliquots (1.0 ml) of each were added to 1.5-ml microcentrifuge tubes. Lysozyme (USA) was added at 10.0 mg ml^{-1}, and total proteins in the pET-30a(+) and Hpa2 supernatants were added to 5.0 mg ml^{-1} (final concentration). The OD_{600} values of all solutions were equally adjusted to 0.800, and the solutions were kept at 25°C for 2 h or 12 h. OD_{600} values were then measured.

The Gram-positive strain *M. luteus* was grown under optimal conditions. It was then treated with the four solutions (pET-30a(+) and Hpa2 supernatants, lysozyme solution, and TE buffer), as described above. Then, the liquids were placed into 1.5-ml microcentrifuge tubes at 25°C for 2 h. The treated cells were then suspended in TE buffer (pH 6.8). For cell fixation, the OD_{600} was adjusted to approximately 2.5 in the presence of 3% glutaraldehyde (Sinopharm Chemical Reagent). Finally, the fixed bacterial cells were observed using transmission electron microscopy (TEM; Electron Microscope Technology Center of Nanjing Agricultural University).

Plant materials and plant inoculations

Chinese cabbage (*Brassica campestris* cv. Beijingxiaoza 56), tobacco (*Nicotiana benthamiana*), tomato (*Lycopersicon esculentum* cv. Jiangsu 14), and pepper (*Capsicum annuum* cv. Sujiao 5) leaves were selected for HR testing. Rice (cv. IR24) was used for pathogenicity testing. Strains *Xoo* $PXO99^A$, 464-16 (*hpa2* mutant), and 712-22 (*hpa2* complement) were used for inoculation. Inoculum concentrations were adjusted to an OD_{600} of 1.0 (approximately 2×10^9 colony-forming units [CFU] ml^{-1}). Leaf-cutting inoculation on rice and needleless syringe infiltration on nonhost plants were used for pathogenicity and HR testing, respectively (Chen and Wang 2003). The infiltration inoculums were all 100 μl. The plants were grown in greenhouses at 28°C (day) and 25°C (night), at 80% humidity. HR and pathogenicity phenotypes were photographed after 24 h or 14 days, respectively.

Bacterial multiplication

Bacterial suspensions (approximately 5×10^5 CFU ml^{-1}) of strains *Xoo* $PXO99^A$, 464-16 (*hpa2* mutant), and 712-22 (*hpa2* complement) were inoculated into rice leaves. Three leaves from each treatment were harvested at 1, 2, 3, and 4 days after inoculation. After the leaves were sterilized with 30% sodium hypochlorite for 3 min, homogenates were prepared in sterile distilled water and plated in NA medium in triplicate. Colonies were counted after 3 days at 28 °C. All statistical data were averaged values from three independent experiments. Data were analyzed using one-way analysis of variance (ANOVA) with a post-hoc multiple-comparisons Tukey's test.

Nucleotide sequence accession numbers

The nucleotide sequences data reported in this paper are registered with the GenBank nucleotide sequence databases

under accession numbers AY139029, EF014415, EF075944, EF075943, and EF075942.

Results

Nucleotide and amino acid sequences analyses

We aligned the full *hpa2* gene of 712 bp (Fig. 1). The *hpa2* sequence contained a promoter region of 148 bp and an ORF of 564 bp. We observed the presence of an imperfect PIP box (TTCGC-N_{15}-TTCGT) in the upstream region of the promoter. Several nucleotide base pairs were changed in strains *Xooc* HAN1, *Xoo* PXO99^{A}, and *Xooc* RS105.

The Hpa2 amino acid sequence was aligned with 11 relatives (Fig. 2). In the 187 amino acids, only Gly and Pro were conserved among all homologous proteins. Glu, Asp, Lys, Arg, Tyr, Cys, and His were determined to be residues of the general acid–base catalysis potential in the enzymes (Wang et al. 2002). These residues were conserved in Hpa2. These residues, however, were different when compared with the 70-kDa soluble LT (SLT70) from *E. coli* (Dijkstra and Thunnissen 1994) and Enterobacteria phage T4 lysozyme (T4L) at similar positions (Fig. 2). The content of the seven residues in the Hpa2, SLT70, and T4L sequences was 30.5%, 28.6%, and 32.3% (Table 2). In comparison, the average content in the seven Hpa2 homologues in *Xanthomonas* and the nine Hrc proteins in *Xoo* MAFF301237 was 31.5% and 22.4%, respectively

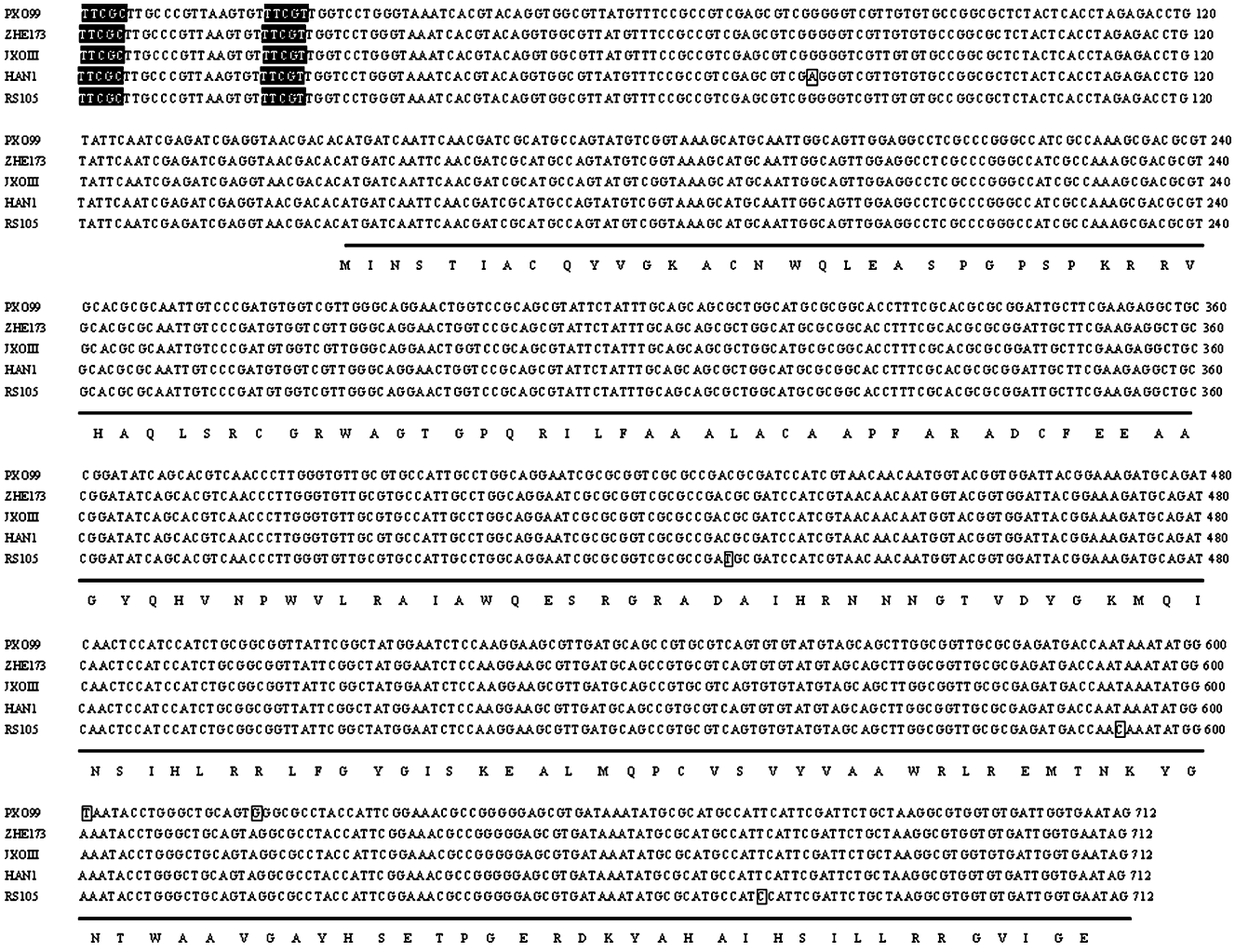

Fig. 1 Sequence alignment of five *hpa2* genes. A conserved sequence of 712 bp among five *hpa2* gene sequences contains a plant-inducible promoter region of 148 bp including an imperfect PIP box TTCGC-N_{15}-TTCGT (*dark gray boxes*). An identical amino acid sequence of 187 amino acids is encoded by the ORFs of 564 bp (*underlined*). *Open squares* indicate the changed bases. Numbering of the five *hpa2* gene sequences: PXO99, *Xanthomonas oxyzae* pv. *oryzae* PXO99 *hpa2*; ZHE173, *X. o.* pv. *oryzae* ZHE173 *hpa2*; JXOIII, *X. o.* pv. *oryzae* JXOIII *hpa2*; HAN1, *X. o.* pv. *oryzicola* HAN1 *hpa2*; RS105, *X. o.* pv. *oryzicola* RS105 *hpa2*

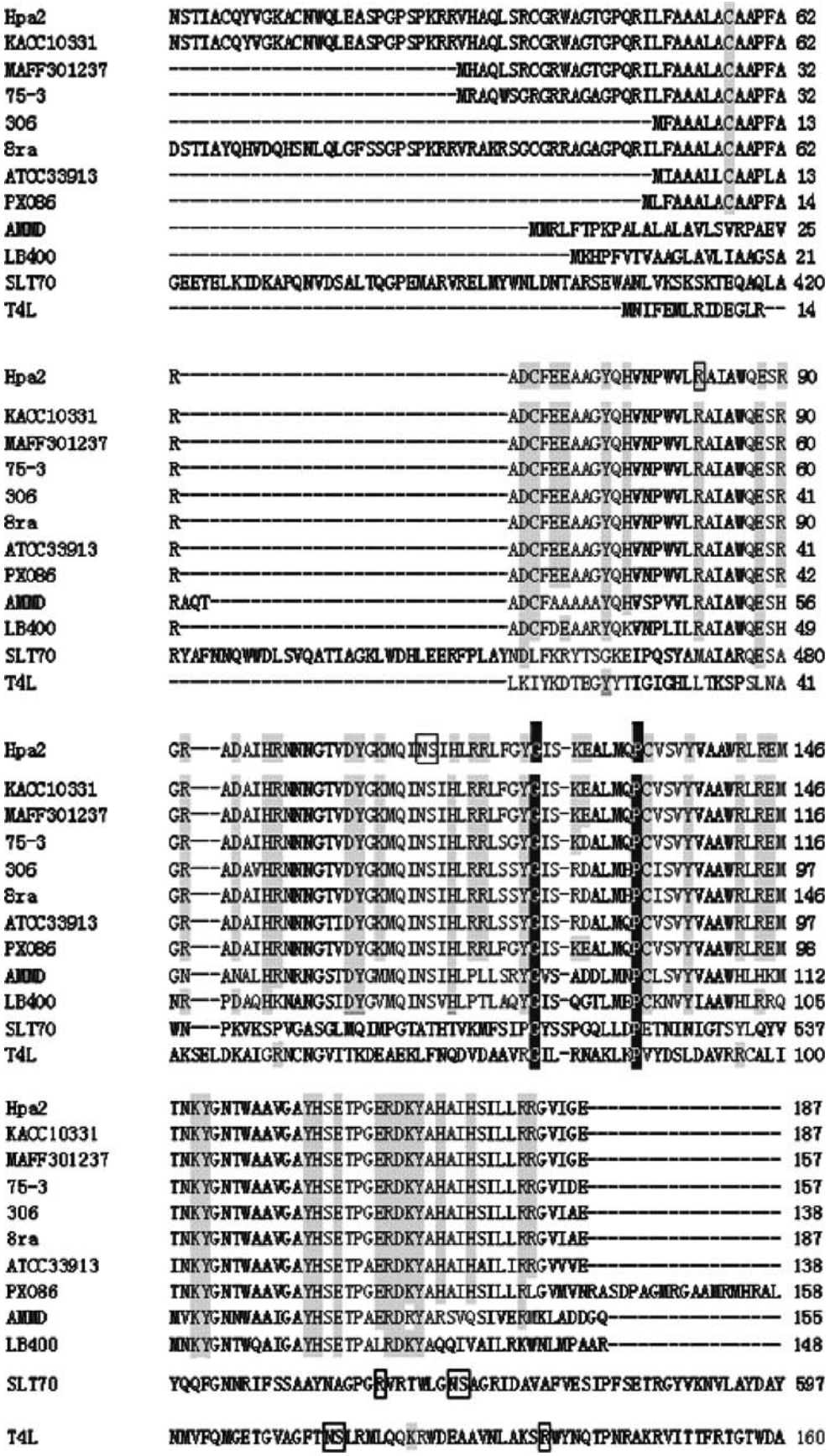
Hpa2
KACC10331
MAFF301237
75-3
306
8ra
ATCC33913
PX086
AMMD
LB400
SLT70
T4L

◀ **Fig. 2** Sequence alignment of Hpa2 protein. The identical amino acids are indicated by the *dark gray boxes*, and the conserved general acid–base catalysis residues in all sequences are indicated by the *light gray boxes*. The peptide-interacting amino acid residues are indicated by the *open squares*. Gaps in the alignment are represented by the *dashes*. *KACC10331*, *X. oryzae* pv. *oryzae* KACC10331 Hpa2 (GenBank accession no. YP_198735); *MAFF301237*, *X. oryzae* pv. *oryzae* MAFF301237 Hpa2 (BAD29978); *75-3*, *X. campestris* pv. *vesicatoria* 75-3 HpaH precursor (AAL78295); *306*, *X. axonopodis* pv. *citri* 306 Hpa2 protein (AAM35308); *8ra, X. axonopodis* pv. *glycines* 8ra HpaH (AAP34333); *ATCC33913*, *X. campestris* pv. *campestris* ATCC 33913 Hpa2 protein (NP_636615); *PXO86*, *X. oryzae* pv. *oryzae* PXO86 Hpa2 precursor (AAF61278); *SLT70*, *E. coli* SLT70 (1QSAA); *T4L*, Enterobacteria phage T4 lysozyme (P00720)

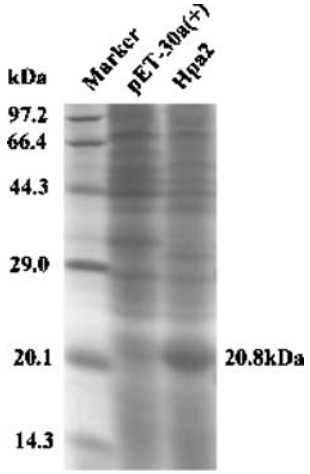

Fig. 3 Expression activity of Hpa2 protein. The band of Hpa2 protein (20.8 kDa) was nearly at a position corresponding marker of 20.1 kDa on the SDS-PAGE image. SDS-PAGE, 15% separating and 5% stacking gels. *Hpa2*, Hpa2 supernatant; *pET-30a(+)*, pET-30a(+) supernatant

(Table 2). Among homologous Hpa2 proteins, matches between residues 65 and 177 (*E* value, 1.2×10^{-15}) indicated that the Hpa2 protein may contain a SLT domain. The side chains of Arg 558, Asn 565, and Ser 566 in SLT70 are positions equivalent to those of the peptide-interacting residues Arg 137, Asn 116, and Ser 117 in T4L (van Asselt et al. 1999). It is intriguing to note that the three residues Arg 82, Asn 112, and Ser 113 in the Hpa2 were the same as those in the T4L at similar positions but were only similar in SLT70 (Fig. 2). These results suggest that there may be differences in catalytic activity or specificity among these proteins.

Hpa2 protein expression and collection

A Hpa2 protein encoded by *hpa2* from the *Xoo* PXO99^{A} strain was expressed in *E. coli* BL21 (DE3) harboring the pEorf564P construct in vitro. The protein consisted of putative 187 amino acids, with a molecular weight of 20.8 kDa (see the corresponding band near the 20.1-kDa marker in Fig. 3). Its isoelectric point (p*I*) was calculated to be 9.62. Consistent with this, we found that in vitro-expressed Hpa2 was a strongly basic protein, and a higher concentration of protein could be obtained in TE buffer with pH 10.1 than at pH 7.2, 8.0, or 9.0 (data not shown).

Table 2 Comparison of Hpa2 general acid–base catalysis residue content

Proteins	Residue contents (%)	Resources
Hpa2	30.5	This study
E. coli SLT70	28.6	GenBank accession no. 1QSAA
Enterobacteria phage T4 lysozyme	32.3	GenBank accession no. P00720
Hpa2 homologues in *Xanthomonas*		
oryzae pv. *oryzae* KACC10331 Hpa2	30.5	GenBank accession no. YP_198735
oryzae pv. *oryzae* MAFF301237 Hpa2	31.2	GenBank accession no. BAD29978
oryzae pv. *oryzae* PXO86 Hpa2 precursor	30.2	GenBank accession no. AAF61278
campestris pv. *campestris* ATCC 33913 Hpa2	31.9	GenBank accession no. NP_636615
campestris pv. *vesicatoria* 75-3 HpaH precursor	31.8	GenBank accession no. AAL78295
axonopodis pv. *citri* 306 Hpa2	32.6	GenBank accession no. AAM35308
axonopodis pv. *glycines* 8ra HpaH	32.1	GenBank accession no. AAP34333
Average	31.5	This study
Hrc proteins in *X. oryzae* pv. *oryzae* MAFF301237		
HrcC	22.5	GenBank accession no. BAD29980.1
HrcT	12.7	GenBank accession no. BAD29981.1
HrcN	27.8	GenBank accession no. BAD29983.1
HrcJ	23.3	GenBank accession no. BAD29986.1
HrcU	27.3	GenBank accession no. BAD29989.1
HrcV	22.2	GenBank accession no. BAD29990.1
HrcQ	21.4	GenBank accession no. BAD29992.1
HrcR	17.8	GenBank accession no. BAD29993.1
HrcS	26.7	GenBank accession no. BAD29994.1
Average	22.4	This study

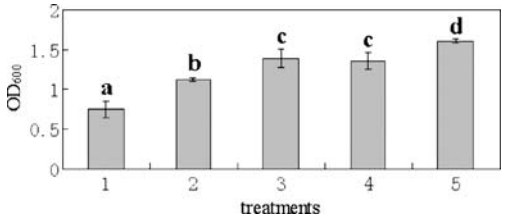

Fig. 4 Secretion activity of Hpa2 protein. Optical density (OD_{600}) value of 564-6 strain solution in the presence of *M. luteus* strain was not significantly different from that of the *M. luteus* strain alone (negative control). Letters *a*, *b*, *c*, and *d* indicate significant differences among the treatments according to one-way ANOVA with the post hoc multiple comparisons Tukey test ($P \leq 0.05$). The *error bars* indicate standard deviations from three replications. Numbering of the five treatments: *1*, Hpa2 supernatant+*Micrococcus luteus* strain; *2*, 564-6 strain+Hpa2 supernatant+*M. Luteus* strain; *3*, 564-6 strain+*M. luteus* strain; *4*, *M. luteus* strain; *5*, 564-6 strain

Hpa2 secretion from *E. coli* cells

To test whether the Hpa2 protein can be released extracellularly without TTSS, that is, if it can serve as a secretory protein from a heterologous cell, we took advantage of the Hpa2 lytic activity to bacterial cell wall and used *M. luteus* as a reporter for Hpa2 presence. After the overexpressing strain 564-6, which bears the *hpa2* gene, was cocultured with *M. luteus* for 12 h, we measured the OD_{600} of the solutions (Fig. 4). The result showed that OD_{600} of 564-6 in the presence of *M. luteus* was not significantly different from the negative control of *M. luteus* alone. Meanwhile, the positive controls (Hpa2+*M. luteus* and 564-6+Hpa2+*M. luteus*) showed a significantly higher OD_{600} value (Fig. 4). This result suggested that *E. coli* cells cannot secrete Hpa2 protein.

Bacteriolysis effect of Hpa2 protein

When we measured bacterial cell integrity by OD_{600} in an in vitro analysis, the Hpa2 protein demonstrated lytic activity against bacterial cells (Fig. 5). We treated bacterial cells with lysozymal solution, Hpa2 supernatant, pET-30a (+) supernatant, and TE buffer solution for 2 and 12 h. The bacterial strains tested were *M. luteus*, *Cms*, *B. subtilis*, *E. coli*, *Xoo* PXO99^{A}, and *Xooc* RS105. At 2 h, the Hpa2 supernatant reduced OD_{600} values in all six strains, compared with the negative control solutions (TE buffer and pET-30a(+) solution). When compared with the positive control lysozymal solution, Hpa2 showed a variable effect. At the 2-h treatment, the Hpa2 solution showed a higher activity than the lysozymal solution in *Cms*, *E. coli*, and *Xoo* PXO99^{A}. It showed a similar activity in *B. subtilis* and *Xooc* RS105 and lower activity in *M. luteus*. After the 12-h treatment, however, the lysozymal solution showed a higher activity than Hpa2 in all strains, except *M. luteus*. This result indicated that Hpa2 may have faster enzymatic kinetics but lower overall activity than lysozymal enzymes, although it is possible that the tested conditions may not reflect the in vivo activity of these enzymes. Because *M. luteus*, *Cms*, and *B. subtilis* are Gram-positive bacteria and *E. coli*, *Xoo* PXO99^{A}, and *Xooc* RS105 are Gram-negative bacteria, the Hpa2 lytic activity may vary in different types of bacteria.

Lytic activity of Hpa2 protein against bacterial cell walls

To further evaluate the Hpa2 lytic effect, we examined the morphology of bacterial cell walls using TEM (Fig. 6). We chose the 2-h treatment based on our previous experiment. Our results showed that the Hpa2 supernatant or lysozyme

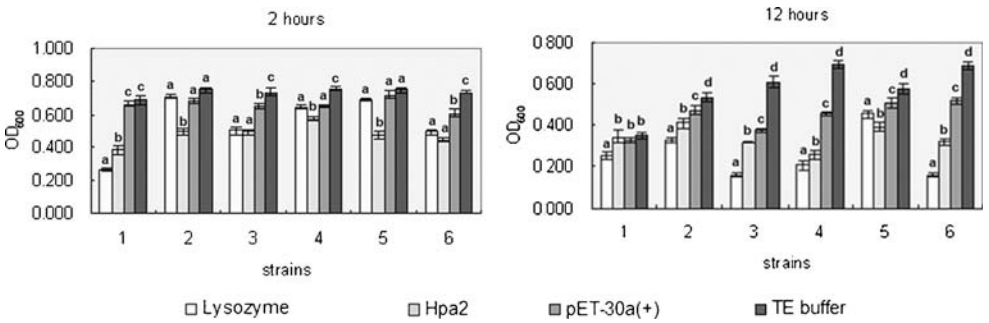

Fig. 5 Bacteriolysis activity of Hpa2 protein. Optical density (OD_{600}) values of six lysed strain solutions were measured after the 2- or 12-h treatment. Letters *a*, *b*, *c*, and *d* indicate significant differences among the treatments. Data analysis was as described in Fig. 4. The data are averages and standard deviations for three independent experiments. Numbering of strains: *1*, *M. luteus*; *2*, *C. michiganense* subsp. *sepedonicum*; *3*, *B. subtilis*; *4*, *E. coli*; *5*, *X. oryzae* pv. *oryzae* PXO99; *6*, *X. oryzae* pv. *oryzicola* RS105. *Lysozyme* Lysozymal solution, *Hpa2* Hpa2 supernatant, *pET-30a(+)* pET-30a(+) supernatant

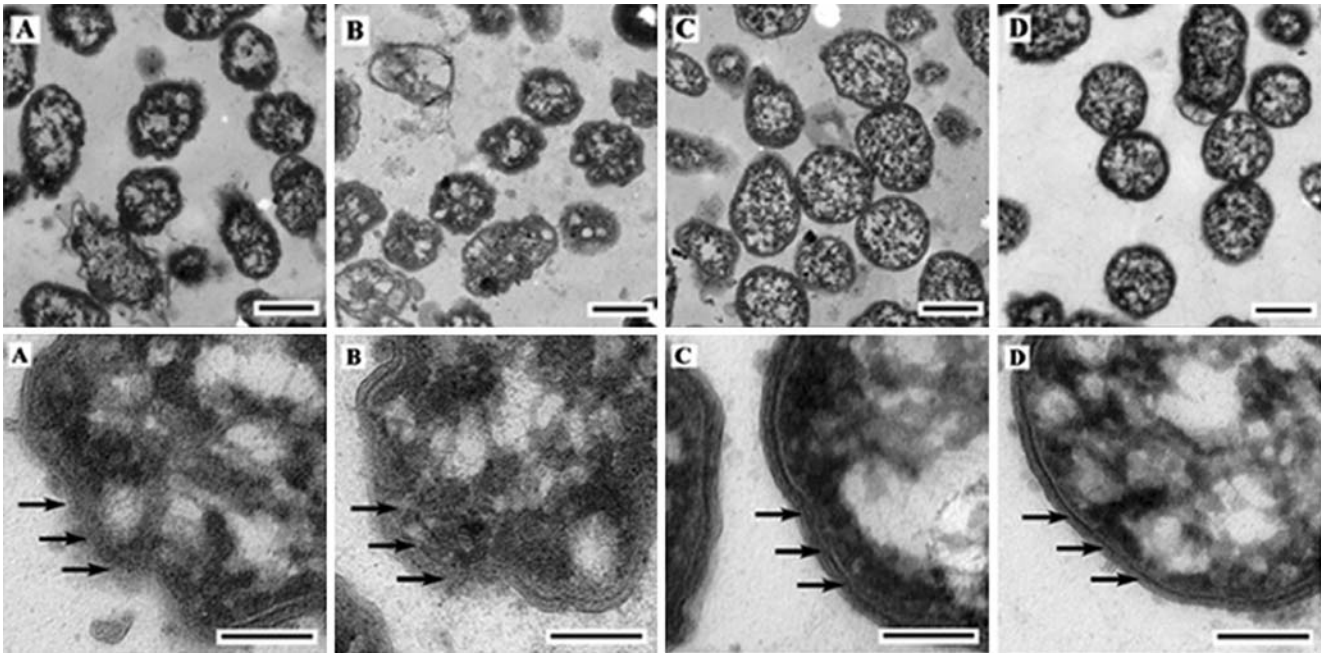

Fig. 6 Hpa2 protein lytic effect on cell walls. The morphologic changes were shown on the transmission electron microscopy images of the lysed *M. luteus* cells. A group of *three arrows* points to the cell wall. Note the protrusive and disrupted portions of the wall in lysozyme solution and Hpa2 supernatant (**a** and **b**). **a** Lysozymal solution, **b** Hpa2 supernatant, **c** pET-30a(+) supernatant, **d** TE buffer. *Scale bars* represent 500 nm for the first list of **a**, **b**, **c**, and **d** or 100 nm for the second list of **a**, **b**, **c**, and **d**

solution lysed the cell walls and caused dramatic roughness and waves in bacterial cells. As controls, cell walls treated with TE buffer or pET-30a(+) supernatant showed much less damage. This result further confirmed the lytic activity of the Hpa2 protein against bacterial cell walls.

A loss-of-function *hpa2* mutant effect on pathogenicity and HR

To evaluate the biological effects of the *hpa2* gene on pathogenicity and HR for bacteria, we generated a loss-of-function insertional mutation in the ORF of *hpa2*, using the suicide vector pKNOCK-Cm (Alexeyev 1999). To test pathogenicity, the wild-type strain *Xoo* PXO99^{A}, the *hpa2* mutant (464-16), and its rescue strain (712-22) were inoculated on rice leaves individually (Fig. 7). Bacterial proliferation was evaluated after 2 days. In the wild-type strain, bacterial cell numbers increased about 1,000-fold. However, the *hpa2* mutation strain only increased about tenfold (Fig. 8). The bacterial count in the rescue transformant strain increased approximately 100-fold at 2 days and nearly reached the level of the wild-type strain at 4 days (Fig. 8). These results suggested that the *hpa2* mutant caused a reduced pathogenicity in the host plant, and the reduced pathogenicity can be partially rescued by

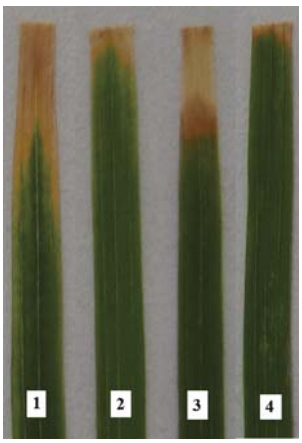

Fig. 7 Phenotypes of rice plant responses to *hpa2* mutant. Inoculation in the *hpa2* mutation strain (*leaf 2*) resulted in a smaller blight than the wild-type strain (*leaf 1*). Leaves were photographed 14 days after inoculation. Numbering of inoculums: *1*, *X. oryzae* pv. *oryzae* PXO99^{A} strain (wild-type); *2*, 464-16 strain (*hpa2* mutant); *3*, 712-22 strain (*hpa2* complement); *4*, water

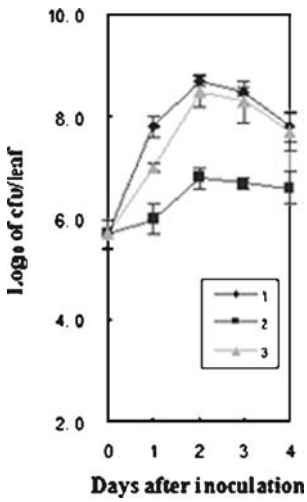

Fig. 8 Effect on growth of *hpa2* mutant in the rice. Bacterial cell numbers (*curve 2*) in the *hpa2* mutation strain was lower about 100-fold than the wild-type strain (*curve 1*) at 2 days. Numbering of inoculums: *1*, *X. oryzae* pv. *oryzae* PXO99^{A} strain; *2*, 464-16 strain (*hpa2* mutant); *3*, 712-22 strain (*hpa2* complement). Data analysis was as described in Fig. 4

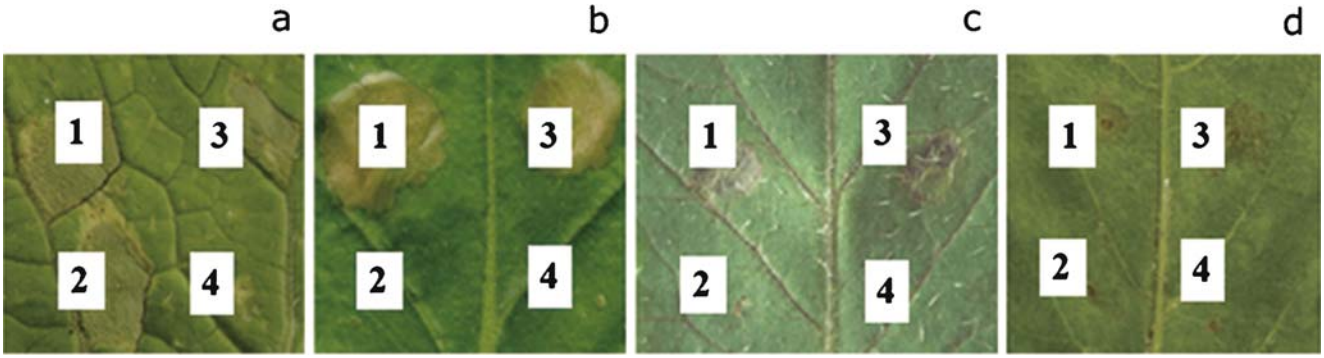

Fig. 9 Phenotypes of nonhost plant responses to *hpa2* mutant. The 464-16 strain (*hpa2* mutant) induced HR in Chinese cabbage but not in tobacco, tomato, or pepper. Leaves were photographed 24 h after inoculation. **a** Chinese cabbage (*B. campestris*, cv. Beijingxiaoza 56); **b** tobacco (*N. benthamiana*); **c** tomato (*L. esculentum*, cv. Jiangsu 14); **d** pepper (*C. annuum*, cv. Sujiao 5). Numbering of inoculums: *1*, *X. oryzae* pv. *oryzae* PXO99^{A} strain; *2*, 464-16 strain (*hpa2* mutant); *3*, 712-22 strain (*hpa2* complement); *4*, water

a copy of the *hpa2* gene. To test HR in nonhost plants, these three strains were inoculated into Chinese cabbage, tobacco, tomato, and pepper leaves. In contrast to the production of HR with the wild-type strain in all these plants, the mutant only induced HR in Chinese cabbage (Fig. 9). Again, the inability of induction of HR in a mutant was rescued by its complementary gene (Fig. 9). These results indicated that the *hpa2* gene was required for HR in some plants but not in others.

Discussion

The *hpa2* gene in *Xoo* was first characterized in 2000 (Zhu et al. 2000). Since then, more genes have been found in other *Xanthomonas* species (Gürlebeck et al. 2006). The predicted proteins encoded by these genes, however, were different in the various bacteria (Table 3). We cloned and compared *hpa2* genes from five *X. oryzae* strains. The amino acid sequences of Hpa2 were identical in these five bacterial strains (Fig. 1). Our results suggest that the *hpa2* gene is highly conserved in *X. oryzae*. Recently, the predicted perfect PIP box (Fenselau and Bonas 1995) and an imperfect PIP box (TTCGC-N_8-TTCGT) in *Xanthomonas* (Oku et al. 2004) were verified as being conserved *cis*-regulatory elements to which the AraC-type transcriptional activator HrpX binds (Koebnik et al. 2006). Thus, a gene containing an imperfect PIP box may be transcribed in a HrpXo-dependent manner (Tsuge et al. 2005). In this study, we found that every *hpa2* gene contained an imperfect PIP box at the same position; thus, they may all belong to the HrpXo regulon.

To test its function, we expressed the Hpa2 protein from *Xoo* PXO99^{A} in vitro. The percentage of residues containing general acid–base catalysis potential was lower in the Hpa2 sequence (30.5%) than in T4L (32.3%) but higher than SLT70 (28.6%; Table 2). These data suggest that the catalytic activity of Hpa2 may be lower than T4L but higher than SLT70. The content of the general acid–base catalysis residues of Hpa2 (30.5%) was close to the average content of the residues of the seven Hpa2 homologues in *Xanthomonas* (31.5%). The average content of the residues of Hrc proteins in the *hrp* gene cluster of *Xoo* MAFF301237 (22.4%), however, was strikingly lower than that of Hpa2 (30.5%), SLT70 (28.6%), or T4L (32.3%), respectively (Table 2). These data also suggest that the Hpa2 could act as a lytic

Table 3 Homology of *X. oryzae* pv. *oryzae* PXO99^{A} Hpa2 protein

Homologues[a]	Size (amino acids)	Identities (%)	Positives (%)	Sources[b]
Xoo KACC10331 Hpa2	187	100	100	YP_198735
Xoo MAFF301237 Hpa2	157	99	100	BAD29978
Xoo PXO86 Hpa2	162	97	99	AAF61278
Xac 306 Hpa2	138	93	97	AAM35308
Xcv 75-3 HpaH	157	93	94	AAL78295
Xcc ATCC33913 Hpa2	138	91	95	NP_636615
Xag 8ra HpaH	187	86	90	AAP34333

[a] *Xoo X. oryzae* pv. *oryzae*, *Xac X. axonopodis* pv. *citri*, *Xcv X. campestris* pv. *vesicatoria*, *Xcc X. campestris* pv. *campestris*, *Xag X. axonopodis* pv. *glycines*

[b] GenBank accession number

protein but likely not a Hrc protein, which functions in the TTSS assembly.

Our experimental data demonstrated Hpa2 lytic activity (Figs. 5 and 6). The supernatant containing the Hpa2 protein showed significantly higher bacterial cell wall lytic activity than TE buffer or its vector control pET-30a(+) supernatant in all six bacterial strains tested. It is interesting to note that the Hpa2 supernatant showed stronger activity than the lysozyme solution at the 2-h treatment in strains such as *Cms*, *E. coli*, and *Xoo* but was lower in the 12-h treatment in *Cms* and *E. coli* (Fig. 5). This suggests that Hpa2 lytic activity may have faster kinetics and lower activity than lysozyme. Alternatively, Hpa2 activity may not be at its maximum under the concentrations or buffer conditions used. Because the bacterial cell wall of *M. luteus* is a natural substrate of lysozyme (Nasr and Fllon 2003; Nakimbugwe et al. 2006), we used it as a special reference strain for analyzing lytic activity. According to the significant differences in OD_{600} after 2 h, we selected *M. luteus* for further cell wall change observations. As nearly 90% of the content of the cell wall is peptidoglycan in *M. luteus* (Brock 1979), the disruption of cell wall was likely caused by multiple damages in the peptidoglycan meshwork. The morphologic change we observed was likely the result of the disrupted cell wall, leading to efflux of intracellular components (Fig. 6).

The autolytic SLT enzyme family (Walderich and Höltje 1991), including SLT70, is a member of the lysozyme-like superfamily. The SLT70 from *E. coli* is an exomuramidase that catalyzes the cleavage of the glycosidic bonds between *N*-acetylmuramic (MurNAc) acid and *N*-acetylglucosamine residues in peptidoglycan (Dijkstra and Thunnissen 1994), the main structural components of the bacterial cell wall. This cleavage is accompanied by the formation of a 1, 6-anhydro bond between the C1 and O6 atoms in the MurNAc acid residue (van Asselt et al. 1999). Such enzymes are capable of locally enlarging gaps in the peptidoglycan meshwork to allow the efficient assembly and anchoring of supramolecular transport complexes in the cell envelope (Koraimann 2003). In the Hpa2 protein, the conserved SLT motif and acid–base catalysis residue content (Table 2) suggest that the catalytic activity of the Hpa2 protein may be the reaction forming a 1,6 anhydro-bond in the MurNAc moiety during peptidoglycan cleavage. Thus, the Hpa2 protein might help assemble the TTSS by enlarging gaps in the peptidoglycan meshwork.

In phytopathogenic bacterial *hrp* gene cluster, the LT or a protein containing a LT domain is likely required in the interaction between TTSS and the host. In *Pseudomonas syringae* pv. *tomato* DC3000 strain, a LT is identified at the 1378 locus, adjacent to the core region of the *hrp* gene cluster (Ferreira et al. 2006). Meanwhile, at the 2678 locus, more distant from the core region, a HopP1 protein including a LT domain, which has the harpin-like property of lacking cysteine, elicits a HR on tobacco leaf (Ferreira et al. 2006; Kvitko et al. 2007). In the *Xcv* 85-10 strain, the efficient secretion of effector proteins requires the contribution of several different Hpa proteins, including the putative LT HpaH, Hpa2 homologue (Gürlebeck et al. 2006; Büttner et al. 2007). The mutation of *hpa2* generated by Zhu et al. (2000) has no apparent effect on pathogenicity; the mutated of *hpaH* had the ability to elicit HR in tomato and Chinese cabbage but not in pepper or tobacco leaves (Kim et al. 2003). In our study, the *hpa2* gene did not fully affect pathogenicity and induced HR in some plants, such as tobacco, tomato, and pepper, but not in Chinese cabbage. These results agree in part with previous observations (Kim et al. 2003; Zhu et al. 2000). This suggests that *hpa2* may contribute to the translocation of some effector proteins that could cause pathogenicity or induce HR, playing a helper role during the interaction between bacteria and plants.

The in vitro protein assay can be applied to study other lysozymal proteins. In combination with mutant analysis in vivo, it provides a simple and powerful technique to understand gene function. Our results suggest that Hpa2 plays an important role in pathogenicity and HR during interaction between TTSS and hosts. Hpa2 may function by contributing to the assembly of the TTSS by enlarging gaps in the peptidoglycan meshwork. Further experiments are still needed to clarify the function of the Hpa2 protein.

Acknowledgments This work was supported by grants from the National Key Basic Research plan of China (no. 2003CB114200 and no. 2006CB101902), the National High Technology Research and Development Program of China (863 Program; no. 2006AA02Z180), and the National Natural Science Foundation of China (no. 30230240). We are particularly grateful to Prof. Gongyou Chen for his critical comments and to Dr. Lei Liu in the USA for his significant and patient help with this manuscript.

References

Alexeyev MF (1999) The pKNOCK series of broad-host-range mobilizable suicide vectors for gene knockout and targeted DNA insertion into the chromosome of Gram-negative bacteria. BioTechniques 26:824–826

Brock TD (1979) Cell wall. In: Brock TD (ed) Biology of microorganisms. 3rd edn. Prentice-Hall, Englewood Cliffs, NJ, pp 25–33

Büttner D, Gürlebeck D, Noël LD, Bonas U (2004) HpaB from *Xanthomonas campestris* pv. *vesicatoria* acts as an exit control protein in type III-dependent protein secretion. Mol Microbiol 54:755–768

Büttner D, Noël L, Stuttmann J, Bonas U (2007) Characterization of the non-conserved *hpaB-hrpF* region in the *hrp* pathogenicity island from *Xanthomonas campestris* pv. *vesicatoria*. Mol Plant Microbe Interact 20:1063–1074

Chen G-Y, Wang J-SH (2003) Exchangeability of two *hrp* gene fragments from *Xanthomonas oryzae* pv. *oryzae* and pv. *oryzicola* for hypersensitive response on tobacco and pathogenicity on rice. Agric Sci Chin 2:975–981

Dijkstra BW, Thunnissen A-MWH (1994) "Holy" proteins II: the soluble lytic transglycosylase. Curr Opin Struck Biol 4:810–813

Fenselau S, Bonas U (1995) Sequence and expression analysis of the *hrpB* pathogenicity operon of *Xanthomonas campestris* pv. *vesicatoria* which encodes eight proteins with similarity to components of the Hrp, Ysc, Spa, and Fli secretion systems. Mol Plant Microbe Interact 8:845–854

Ferreira AO, Myers CR, Gordon JS, Martin GB, Vencato M, Collmer A, Wehling MD, Alfano JR, Moreno-Hagelsieb G, Lamboy WF, DeClerck G, Schneider DJ, Cartinhour SW (2006) Whole-genome expression profiling defines the HrpL regulon of *Pseudomonas syringae* pv. *tomato* DC3000, allows de novo reconstruction of the Hrp *cis* clement, and identifies novel coregulated genes. Mol Plant Microbe Interact 19:1167–1179

Galán JE, Collmer A (1999) Type III secretion machines: bacterial devices for protein delivery into host cells. Science 284:1322–1328

Gürlebeck D, Thieme F, Bonas U (2006) Type III effector proteins from the plant pathogen *Xanthomonas* and their role in the interaction with the host plant. J Plant Physiol 163:233–255

Horino O (2002) Studies on resistance mechanisms of rice against bacterial blight caused by *Xanthomonas oryzae* pv. *oryzae*. J Gen Plant Pathol 68:253–256

Hueck CJ (1998) Type III protein secretion systems in bacterial pathogens of animals and plants. Microbiol Mol Biol Rev 62:379–433

Huguet E, Hahn K, Wengelnik K, Bonas U (1998) *HpaA* mutants of *Xanthomonas campestris* pv. *vesicatoria* are affected in pathogenicity but retain the ability to induce host-specific hypersensitive reaction. Mol Microbiol 29:1379–1390

Kim JG, Park BK, Yoo CH, Jeon E, Oh J, Hwang I (2003) Characterization of the *Xanthomonas axonopodis* pv. *glycines* Hrp pathogenicity island. J Bacteriol 185:3155–3166

Koebnik R, Krüger A, Thieme F, Urban A, Bonas U (2006) Specific binding of the *Xanthomonas campestris* pv. *vesicatoria* AraC-type transcriptional activator HrpX to plant-inducible promoter boxes. J Bacteriol 188:7652–7660

Koraimann G (2003) Lytic transglycosylases in macromolecular transport systems of gram-negative bacteria. Cell Mol Life Sci 60:2371–2388

Kumar RS, Sakthivel N (2001) Exopolysaccharides of *Xanthomonas* pathovar strains that infect rice and wheat crops. Appl Microbiol Biotechnol 55:782–786

Kvitko BH, Ramos AR, Morello JE, Hye-Sook Oh H-S, Collmer A (2007) Identification of harpins in *Pseudomonas syringae* pv. *tomato* DC3000, which are functionally similar to HrpK1 in promoting translocation of type III secretion system effectors. J Bacteriol 189:8059–8072

Lee BM, Park YJ, Park DS, Kang HW, Kim JG, Song ES, Park IC, Yoon UH, Hahn JH, Koo BS, Lee GB, Kin H, Park HS, Yoon KO, Kim JH, Jung CH, Koh NH, Seo JS, Go SJ (2005) The genome sequence of *Xanthomonas oryzae* pathovar *oryzae* KACC10331, the bacterial blight pathogen of rice. Nucleic Acids Res 33:577–586

Li P, Lu X, Shao M, Long J, Wang J (2004) Genetic diversity of Harpins from *Xanthomonas oryzae* and their activity to induce hypersensitive response and disease resistance in tobacco. Sci China Ser C Life Sci 47:461–469

Nakimbugwe D, Masschalck B, Atanassova M, Abebetch ZB, Michiels CW (2006) Comparison of bactericidal activity of six lysozymes at atmospheric pressure and under high hydrostatic pressure. Int J Food Microbiol 108:355–363

Nasr NM, Fllon AM (2003) Detection of lysozyme-like enzymatic activity secreted by an immune-responsive mosquito cell line. J Invertebr Pathol 82:162–166

Niño-Liu DO, Ronald PC, Bogdanove AJ (2006) *Xanthomonas oryzae* pathovars: model pathogens of a model crop. Mol Plant Pathol 7:303–324

Ochiai H, Inoue Y, Takeya M, Sasaki A, Kaku H (2005) Genome sequence of *Xanthomonas oryzae* pv. *oryzae* suggests contribution of large number of effector genes and insertion sequences to its race diversity. Jpn Agric Res Q 39:275–287

Oku T, Tanaka K, Iwamoto M, Inoue Y, Ochiai H, Kaku H, Tsuge S, Tsuno K (2004) Structural conservation of the *hrp* gene cluster in *Xanthomonas oryzae* pv. *oryzae*. J Gen Plant Pathol 70:159–167

Sambrook J, Russell DW (2001) Appendix 8: commonly used techniques. In: Sambrook J, Russell DW (eds) Molecular cloning: a laboratory manual. 3rd edn. Cold Spring Harbor Laboratory, New York, pp A8.40–A8.47

Sugio A, Yang B, White FF (2005) Characterization of the *hrpF* pathogenicity peninsula of *Xanthomonas oryzae* pv *oryzae*. Mol Plant Microbe Interact 18:546–554

Tsuge S, Terashima S, Furutani A, Ochiai H, Oku T, Tsuno K, Kaku H, Kubo Y (2005) Effects on promoter activity of base substitutions in the *cis*-acting regulatory element of HrpXo regulons in *Xanthomonas oryzae* pv. *oryzae*. J Bacteriol 187:2308–2314

van Asselt EJ, Thunnissen A-MWH, Dijkstra BW (1999) High resolution crystal structures of the *Escherichia coli* lytic transglycosylase SLT70 and its complex with a peptidoglycan fragment. J Mol Biol 291:877–898

Walderich B, Höltje JV (1991) Subcellular distribution of the soluble lytic transglycosylase in *Escherichia coli*. J Bacteriol 173:5668–5676

Wang J, Zhu S, Xu C (2002) Biochemistry, vol. 1. 3rd edn. Higher Education, Beijing, pp 390–392 (in Chinese)

Wang X, Li M, Zhang J, Zhang Y, Zhang G, Wang J (2007) Identification of a key functional region in harpins from *Xanthomonas* that suppresses protein aggregation and mediates harpin expression in *E. coli*. Mol Biol Rep 34:189–198

Zhao B, Ardales EY, Raymundo A, Bai J, Trick HN, Leach JE (2004) The *avrRxo1* gene from the rice pathogen *Xanthomonas oryzae* pv. *oryzicola* confers a non-host defense reaction on maize with resistance gene *Rxo1*. Mol Plant Microbe Interact 17:771–779

Zhu W, Magbanua MM, White FF (2000) Identification of two novel *hrp*-associated genes in the *hrp* gene cluster of *Xanthomonas oryzae* pv. *oryzae*. J Bacteriol 182:1844–1853

Zou L, Wang X, Xiang Y, Zhang B, Li Y, Xiao Y, Wang J, Walmsley AR, Chen G (2006) Elucidation of the *hrp* clusters of *Xanthomonas oryzae* pv. *oryzicola* that control the hypersensitive response in non-host tobacco and pathogenicity in susceptible host rice. Appl Environ Microbiol 72:6212–6224